tRNase Z Catalysis and Conserved Residues on the Carboxy Side of the His Cluster †

3 **AUTHORS**, INCLUDING:

Shay Karkashon

6 PUBLICATIONS   26 CITATIONS

SEE PROFILE

Angela Reeves (Hopkinson)

Abbott Laboratories

7 PUBLICATIONS   205 CITATIONS

SEE PROFILE

tRNase Z Catalysis and Conserved Residues on the Carboxy Side of the His Cluster

Shay Karkashon[@], **Angela Hopkinson**[#], and **Louis Levinger**[*]
York College of The City University of New York 94-20 Guy R. Brewer Blvd. Jamaica, NY 11451

Abstract

tRNAs are transcribed as precursors and processed in a series of required reactions leading to aminoacylation and translation. The 3′ end trailer can be removed by the pre-tRNA processing endonuclease tRNase Z, an ancient, conserved member of the β-lactamase superfamily of metal-dependent hydrolases. The signature sequence of this family, the His domain (HxHxDH, Motif II), and histidines in Motifs III and V and aspartate in Motif IV contribute seven side chains for coordination of two divalent metal ions. We previously investigated the effects on catalysis of substitutions in Motif II, and in the PxKxRN loop and Motif I on the amino side of Motif II. Herein we present the effects of substitutions on the carboxy side of Motif II within Motifs III, IV, the HEAT and HST loops and Motif V. Substitution of the Motif IV aspartate reduces catalytic efficiency more than 10,000-fold. Histidines in Motif III, V and the HST loop are also functionally important. Strikingly, replacement of Glu in the H**E**AT loop with Ala reduces efficiency by ~1000-fold. Proximity and orientation of this Glu side chain relative to His in the HST loop and the importance of both residues for catalysis suggest that they function as a duo in a proton transfer at the final stage of reaction, characteristic of the tRNase Z class of RNA endonucleases.

INTRODUCTION

tRNAs are transcribed as precursors with a 5′ end leader and a 3′ end trailer which must be removed in the course of maturation before aminoacylation and translation. tRNase Z is a tRNA-specific 3′ end endonuclease found in all eukaryotes and archaea and about half of bacteria (reviewed in Vogel et al., 2005), and is thus surmised to be of ancient origin which predates divergence of the kingdoms. CCA at the 3′ end of mature tRNA is not encoded in the tRNA genes of archaea, eukaryotes and some bacteria; in these cases, CCA must be post-transcriptionally added to the discriminator base by CCA-adding enzyme. tRNase Z leav es a 3′-OH after the discriminator, rendering the tRNA product available for CCA addition.

Specificity of tRNase Z for tRNA is due to the flexible domain (de la Sierra-Gallay et al., 2005; Schilling et al., 2005) which is located outside the body of the enzyme and binds the elbow of the tRNA (de la Sierra-Gallay et al., 2006), distant from the 3′ end of the acceptor stem. Additional contacts with the acceptor stem and 3′ end trailer (de la Sierra-Gallay et al., 2005, 2006; Zareen et al., 2006) suggest a structural basis for the CCA anti-determinant, which prevents tRNA from cycling back from CCA addition through tRNase Z cleavage (Nashimoto, 1997; Mohan et al., 1999; Pelligrini et al., 2003).

[*]to whom correspondence should be addressed: Phone: 718-262-2704 FAX: 718-262-2652 Email: louie@york.cuny.edu.
[@]Present Addresses: Albert Einstein College of Medicine, Department of Hematology, Forcheimer Building, Bronx, New York 10461;
[#]Department of Microbiology and Immunology, 5641 Medical Sciences Building II, 1150 W. Medical Center Dr., Ann Arbor, MI 48109-0620

Before the expression and characterization of tRNase Z (Schiffer et al., 2002), its gene was identified as a candidate human prostate cancer susceptibility gene (ELAC2; Tavtigian et al., 2001). tRNase Z can be encoded as a long form (tRNase Z^L, found only in eukaryotes) or as a short form (tRNase Z^S, the only form in bacteria and archaea); both long and short forms are present, encoded by different genes, in humans and other chordates. ELAC2 encodes tRNase Z^L (Tavtigian et al., 2001; Takaku et al., 2003). *S. cerevisiae*, *C. elegans* and *D. melanogaster* encode only tRNase Z^L. tRNase Z^L was hypothesized to have emerged as a tandem gene duplication of tRNase Z^S (Tavtigian et al., 2001) and while tRNase Z^S functions as a homodimer (Spath et al., 2005; de la Sierra-Gallay et al., 2005), tRNase Z^L presumably functions as a monomer. After the hypothesized tandem gene duplication, the amino half of tRNase Z^L retained the flexible domain and lost the active site, while the carboxy region retained the catalytic center and lost the flexible domain. Coinciding with evolutionary divergence of the halves of tRNase Z^L, human tRNase Z^L achieved a 1,700-fold greater catalytic efficiency than tRNase Z^S, by means of an increase in k_{cat} and a decrease in k_M (Yan et al., 2006).

tRNase Z^L has many desirable characteristics but no structure for a eukaryotic tRNase Z^L is currently available. It is therefore necessary to rely on bacterial tRNase Z^S for structures (de la Sierra-Gallay et al., 2005; Iishi et al., 2005; Kostelecky et al., 2006). This is shown to be valid by sequence conservation between tRNase Z^L and tRNase Z^S in functionally important loops (Figure 1).

tRNase Z is a member of the β-lactamase superfamily of metal-dependent hydrolases, the signature sequence of which is the His cluster (-HxHxDH-; Motif II). Motif II collaborates with Motifs III, IV and V on the carboxy side of Motif II; seven amino acid side chains coordinate two divalent metal ions. Some of the effects of substitutions in Motif II on catalysis (Zareen et al., 2005) presumably arise from perturbation of metal ion binding. In addition to Motifs II-V, sequence alignments (Figure 1), tRNase Z structure (Figure 2) and mutagenesis studies (Vogel et al., 2004; Spath et al., 2005) suggest that residues in two conserved loops located between Motifs IV-V, referred to here as HEAT and the HST loop based on their most conserved sequences in tRNase Z^Ls (Figure 1D, E), may also be involved in catalysis.

Using *D. melanogaster* tRNase Z (a long form), we performed Ala-scanning mutagenesis through five conserved loops on the carboxy side of Motif II (Motifs III, IV, HEAT, HST and Motif V) and analyzed the pre-tRNA processing kinetics of the expressed variants. Relatively minor effects on k_M suggest the general absence of strong binding residues in this part of the molecule. On the other hand, a number of substitutions reduce k_{cat} by three to four orders of magnitude. Results are consistent with the function of histidines in motifs III and V and aspartate in Motif IV in metal ion coordination necessary for catalysis. Interestingly, they also support a function for glutamate in the H**E**AT loop and histidine in the **H**ST loop that could be central to the final step of catalysis. A structurally homologous Glu – His duo is found in human CPSF-73 (Mandel et al., 2006), a member of the metallo-beta-lactamase family which has recently been suggested to be the long-sought 3′ end endonuclease for pre-mRNA (including pre-histone mRNA) maturation (Ryan et al., 2004; Dominski et al., 2005; Mandel et al., 2006).

METHODS

tRNase Z expression and mutagenesis

The *D. melanogaster* tRNase Z cDNA (Accession # AY119279) was first subcloned and expressed using baculovirus from an internal methionine at residue 24 suggested to be the translation start for the nuclear form of the enzyme (Dubrovsky et al., 2004). Residues are thus numbered from +1 for this methionine (Zareen et al., 2005), hence H500 for the central histidine

of Motif II (Figure 1A). Overlap extension PCR was used to prepare ~550 bp inserts with substitution of GCC (Ala) codons at specific positions (seven in Motif III, seven in Motif IV, four in the HEAT loop [the A of HEAT was substituted with a T], ten in the HST loop, and seven in Motif V; Figure 1B–F). The unique internal Bpu10I site (nt 1863) and the introduced Xho site directly following the natural termination codon (nt 2407–2409) were used for subcloning into the tRNase Z cDNA pFastbac HTA (Invitrogen) transfer vector plasmid as previously described (Zareen et al., 2005). Accuracy of construction was confirmed by sequencing (Herbert Irving Comprehensive Cancer Center core facility, Columbia College of Physicians and Surgeons). Baculovirus transfer, expression in insect Sf9 cells and nickel chelate affinity purification of soluble tRNase Z were performed as previously described (Zareen et al., 2005). Enzyme concentrations were determined using the Biorad dye reagent and confirmed by gel electrophoresis and fluorescent staining (Figure 3B).

Construction and preparation of substrate

D. melanogaster pre-tRNA^{His} that was previously used as a tRNase Z substrate (Frendewey et al., 1985; Levinger et al., 1995) has a long structured 3′ end trailer. To investigate the generality of kinetic parameters obtained with pre-tRNA^{His}, we constructed a canonical tRNA with a 17 nt 3′ end trailer, *D. melanogaster* tRNA$^{Arg(UUA)}$ (Figure 1A; Accession # L09202, nt 1197–1286), by extension PCR using long overlapping primers. Because of a naturally occurring internal BamHI site in the tRNA^{Arg} sequence, EcoRI and HindIII sites were used for subcloning. A T7 promoter and hammerhead ribozyme were used for accurate and efficient production of pre-tRNA^{Arg} with a mature 5′ end (Fechter et al., 1998). After sequencing to confirm accuracy of construction, unlabelled runoff RNA was prepared by T7 transcription of a template DraI digest (to obtain –UUU at the 3′ end of the 3′ end trailer), cleaved with the hammerhead and gel purified. Pre-tRNA^{Arg} was 5′-endlabeled with λ-^{32}P-ATP and polynucleotide kinase and repurified.

Kinetics of tRNase Z processing

For kinetic experiments, a low, constant concentration of labeled substrate was supplemented with a varied concentration of unlabeled pre-tRNA^{Arg}. Processing efficiencies were initially determined using labeled pre-tRNA^{Arg} with a 17 nt 3′ end trailer at a concentration of approximately 10^{-10} M, between one and two orders of magnitude lower than the lowest k_M observed (Tables 1–5), so as to approximate zero-order kinetics, in which the % product/minute of reaction (V/[S]) evaluated early in a reaction time course is proportional to V (data not shown). More than 50% of the substrate could be processed if sufficient wild type enzyme was used (not shown); reproducible kinetic parameters were obtained with the lowest possible concentration of each variant enzyme. Wild type tRNase Z was used at a concentration of 25 pM, at least 1,000 times lower than has been used by other laboratories (e.g. Takaku et al., 2003;Spath et al., 2005). Enzyme concentrations were adjusted as necessary based on results of variant processing efficiencies determined without added unlabeled substrate. While % product/minute (V/[S]) decreases with increasing [S], V (obtained by multiplying V/[S] by [S]) increases with [S]. The substrate concentration range (usually 2 –100 nM) was adjusted so that k_M fell in the middle of the [S] range for each tRNase Z variant. V_{max} (obtained from Eadie-Hofstee plots; Figure 3C) was converted to k_{cat} by multiplying by [E]. Enzyme concentration was obtained from the original wild type and variant enzyme stocks (Biorad assay); these were diluted to substocks (2 μg/μL, equivalent to 2.5×10^{-5} M). In the first tube of a dilution series, enzymes were diluted 1:10 to 200 ng/μL. To refine the estimation of [E} in kinetic experiments, 2.5 μL of this dilution was electrophoresed on a protein gel (Figure 3B). All variant enzymes were used in at least two kinetic experiments; each time kinetics was performed on a set of variants, a parallel experiment with wild type tRNase Z was included. Comparisons to determine relative k_{cat}/k_M were made between variant and wild type tRNase

Zsperformed on the same day. The wild type tRNase Z data presented (line 1 in Table 1) are the means of thirty kinetic experiments.

Multiple sequence alignments

Multiple sequence alignments were prepared using Clustalw and displayed using GeneDoc.

Structure model display of loops on the carboxy side of Motif II

The tRNase Z structure model (Figure 2, 5A; de la Sierra-Gallay et al., 2005; PDB #1Y44) and homologous residues in human CPSF-73 (Figure 5B;Mandel et al., 2006; PDB #2I7T) were visualized using Cartoon and Side Chains in PyMol (Delano, 2002).

RESULTS AND DISCUSSION

Conserved loops on the carboxy side of Motif II

In the tRNase Z branch of the β-lactamase superfamily, binding of two zinc ions is coordinated by four residues in the signature His domain (Figure 1A; Motif II, -HxHxDH-; the central histidine is H500), with additional bonds contributed by the Motif III histidine, Motif IV asparatate and Motif V histidine (H583, D610, H668 in *Dme*, respectively; •s in Figure 1B, C, F; reviewed in Callebaut et al., 2002; Dominski, 2007). The HEAT loop (Figure 1D) and the HST loop (Figure 1E) are also conserved. Informative Ala scans through Motif II (Zareen et al., 2005) and through the PxKxRN loop and Motif I region on the amino side of Motif II (Zareen et al., 2006) led to the undertaking of single residue scans through five conserved loops (a total of 35 residues; Figure 1B-F) on the carboxy side of Motif II.

Reaction kinetics of tRNase Z variants with Ala substitutions through conserved loops on the carboxy side of Motif II

A new substrate (*D. melanogaster* pre-tRNA[Arg]; Figure 3A) with a shorter, more typical 3′ end trailer (17 nt) than the previously analyzed pre-tRNA[His] (see Methods) gives kinetic parameters with wild type tRNase Z (left upper panel in Figure 3C; cf D; top line in Table 1) similar to those previously reported using pre-tRNA[His] as substrate (Zareen et al., 2005, 2006). These experiments were performed with a wild type *D. melanogaster* tRNase Z (a tRNase Z[L]) concentration of 25 pM, at least 1,000 times lower enzyme concentration than was used by others. The higher reaction efficiencies may be accounted for by the use of tRNase Z[L], baculovirus expression, and careful optimization of reaction conditions.

Gel data and Eadie-Hofstee plots used for kinetic analysis of the first three residues in the Motif III region (Figure 3B-D) include the Motif III histidine. The Michaelis constant (k_M) is related to a dissociation constant; with minor exceptions, k_M for the variants is similar to the mean wild type k_M value of 15 nM, suggesting that residues involved with metal ion binding and catalysis are not directly involved with substrate recognition and binding, in agreement with previous results for Motif II (Zareen et al., 2005).

Kinetic analyses on all the residues analyzed with Ala substitutions in Motifs III, IV, the HEAT and HST loops and Motif V (Figure 1B-F) were performed using the same procedures (not shown) and results are presented in Tables 1A-E and Figure 4A-E, respectively. Eadie-Hofstee plots display similar slopes (-k_M; Figure 3D). Slight variations in k_M modulate the values for k_{cat}/k_M, however (compare the values in Table 1 for subtle differences). Values in Figure 4 differ from those that would be calculated from the data presented in Table 1 because k_{cat} and k_M for wild type tRNase Z used to calculate k_{cat}/k_M relative to wild type (column 5 in Table 1) and to plot the bar graphs (Figure 4) varied from day to day.

The main term that influences k_{cat} in these experiments is the concentration of variant tRNase Z (shown above the processing gel panels; Figure 3C). Some Ala substitutions were so impairing (e.g. H583; see Figure 3C, D) that even at a much higher variant enzyme concentration than was used for the wild type, a substantially reduced percentage of product and therefore, V_{max}, was obtained. In these instances, low V_{max} and high [E] both contribute to measured impairment. Of all the Motif III residues scanned, only H583A substantially impaired catalysis (almost 1000-fold; Table 1A, Figure 4A).

The Motif IV aspartate and the region surrounding it (Table 1B; Figure 4B) are different from Motif III (cf Table 1A; Figure 4A) in interesting ways. The effect of substitution of D610 with alanine is greater, a more than 10,000-fold reduction in catalytic efficiency, consistent with D610 bridging two metal ions (Vogel et al., 2004;de la Sierra-Gallay et al., 2005). Slight but reproducible reductions in k_M arise from Ala substitutions throughout the entire loop. Repulsion between acidic D610 and phosphates in the backbone of the substrate could be endemic to tRNase Z catalysis; decreased repulsion due to replacement or repositioning of D610 could allow more stable penetration of the 3' end trailer into the active site.

The Glu in H**E**AT (Figure 1D, 2D) contributes to catalysis (Table 1C, Figure 4C). Substitution of E630 with alanine causes a 1000-fold decrease in k_{cat} and catalytic efficiency while substitution of H629 has relatively little effect (Table 1C, Figure 4C). This is the first report of a substantial effect on catalysis arising from substitution of this conserved Glu. A ~2-fold reduction was observed in a previous report on domains of *Arabidopsis thaliana* tRNase Z^S, (Spath et al., 2005). Detailed comparison between present results and reports from other groups is not possible, but the more than 1000-fold greater catalytic efficiency of baculovirus expressed, soluble fruit fly tRNase Z^L than the tRNase Z^L and tRNase Z^S used in functional studies by other labs greatly increases the analytical range; such differences in materials and methods could contribute to recognition of the functional importance of E in HEAT.

Histidine of the HST loop (Figure 1E; Figure 2, Table 1D, Figure 4D) has previously been suggested to be important for catalysis and has been substituted before (Vogel et al., 2004; Spath et al., 2005; Minagawa et al., 2006). Substitution of H646 with alanine reduces catalytic efficiency more than 10,000-fold (Table 1D, Figure 4D). Various arguments have been made that histidine of the HST loop is directly involved in catalysis. Mn^{++} rescue of catalysis by *T. maritima* tRNase Z mutants was used as the primary argument that the Motif II aspartate and histidine of the HST loop (which could not be rescued) provide the engine for general acid/base catalysis (Minagawa et al., 2006). While these results led to a plausible model, only a slight effect of Mn^{++} on catalysis by *D. melanogaster* tRNase Z was found with any of the corresponding substituted variants (data not shown). As previously observed (see below), the side chain of E630 is oriented toward H646 (E231 and H247 in *B. subtilis* tRNase Z; E204 and H396 in human CPSF-73; Figure 5 and Mandel et al., 2006) at the correct position for an H-bond between them to make H646 more acidic, increasing its ability to donate a proton to complete the 3′-O**H** of the tRNA product.

Histidine 668 in Motif V contributes a coordination bond for metal ion binding and the H668A substitution reduces catalytic efficiency more than 1000-fold (Table 1E, Figure 4E). Interestingly, substitutions surrounding the Motif V histidine produce a gradual rise and fall in efficiency, unlike those in Motif IV, suggesting that Motif V is less rigid than Motif IV and HEAT.

A homolog of the Glu^{231}-His^{247} duo in human CPSF-73

Structure, conserved sequence and catalysis with variant enzymes (Vogel et al., 2004; Spath et al., 2005; Minegawa et al., 2006) suggest that H247 may contribute directly to catalysis and E231 has the right charge and position to transform H247 into a general acid for catalysis

(shown in Figure 5A in a view similar to that in Figure 2H; de la Sierra-Gallay et al., 2005, 2006). The structurally homologous position of a Glu-His duo with relation to the active site of human CPSF-73 (Figure 5B; Mandel et al., 2006, cfA) suggests that this protein, recently suggested to be the long-sought endonuclease responsible for the cleavage step in 3' end polyadenylation and pre-histone mRNA maturation (Ryan et al., 2004; Dominski et al., 2005; Mandel et al., 2006) works by the same mechanism (Mandel et al., 2006).

Both tRNase Z and CPSF-73 have a metallo-β-lactamase domain; additionally, CPSF-73 has a β-CASP domain, making it a member of a related branch of the β-lactamase superfamily (Callebaut et al., 2002; Dominski, 2007). The β-CASP (metallo-**β**-lactamase, **C**PSF, **A**rtemis, **S**nm1, **P**so2) family is characterized by three motifs (A: Asp or Glu; B, C: His) which overlap the five motifs (I-V) of the β-lactamase superfamily. Curiously, the β-CASP domain of CPSF (residues 209–394) interrupts the β-lactamase domain (residues 1–208, 395–460). CPSF-73 is not included in the selected alignments (Figure 1) because its sequence in these loops is not nearly as conserved. Indeed, functionally equivalent residues in tRNase Z and CPSF-73 beyond Motif IV were only identified based on the CPSF-73 structure (Mandel et al., 2006): Glutamate 204, located between the end of the β-lactamase domain and the start of the β-CASP domain (Motif A) is equivalent to glutamate in HEAT; His 396 in the linker just beyond the carboxy end of the β-CASP domain of CPSF-73 (Motif B) is equivalent to H of the HST loop; His 418, part of the β-lactamase domain beyond the carboxy end of the β-CASP domain of CPSF-73 (Motif C), is equivalent to the Motif V histidine. Despite a rather low overall sequence identity between tRNase Z and CPSF-73 (<20%), structural homology of the Glu-His duo (Figure 5) extends to include the active site residues in CPSF-73, H71, H73, D75, H76 (Motif II), H158 (Motif III), D179 (Motif IV) and H418 (Motif V), which are virtually superimposable on those of tRNase Z (not shown).

Metalloprotein architecture and catalysis

Substitution of any one of the seven residues involved in metal ion coordination results in a reduced k_{cat} of between 500 and >10,000-fold (Zareen et al., 2005; Figures 4A,B,E). A divalent metal can coordinate OH$^-$ that serves to initiate nucleophilic attack on phosphate at the 3′ side of the scissile bond. This OH$^-$ has been suggested to be produced by D502 (D67 in *B. subtilis*), which could remove a proton from water in addition to contributing a coordination bond to Zn^{++}. In the final step of strand scission, a proton must be donated to produce the 3′-O**H** on ribose of the discriminator base; H646 (H247) of the HST loop could be rendered capable of donating this proton due to its interaction with E630 (E231) of the HEAT loop (Mandel et al., 2006). tRNase Z and CPSF-73, both RNA endonucleases in the β-lactamase family, use the metalloprotein components of Motifs II -V architecturally and for catalysis. E and H residues that are not involved in metal ion coordinationcrucially participate.

Acknowledgements

References

Callebaut I, Moshous D, Mornon J-P, de Villartay J-P. Metallo-3-lactamase fold within nucleic acids processing enzymes: the 3-CASP family. Nucleic Acids Res 2002;30:3592–3601. [PubMed: 12177301]

de la Sierra-Gallay IL, Pellegrini O, Condon C. Structural basis for substrate binding, cleavage and allostery in the tRNA maturase RNase Z. Nature 2005;433:657–661. [PubMed: 15654328]

de la Sierra-Gallay IL, Mathy N, Pellegrini O, Condon C. Structure of the ubiquitous 3′ processing enzyme RNase Z bound to transfer RNA. Nat Struct Mol Biol 2006;13:376–377. [PubMed: 16518398]

DeLano, WL. The PyMOL Molecular Graphics System on World Wide Web. 2002. http://www.pymol.org

Dominski Z, Yang XC, Marzluff WF. The polyadenylation factor CPSF-73 is involved in histone-pre-mRNA processing. Cell 2005;123:37–48. [PubMed: 16213211]

Dominski Z. Nucleases of the metallo-3-lactamase family and their role in DNA and RNA metabolism. Crit Rev Biol & Mol Biol 2007;42:67–93.

Dubrovsky EB, Dubrovskaya VA, Levinger L, Schiffer S, Marchfelder A. *Drosophila* RNase Z processes mitochondrial and nuclear pre-tRNA 3′ ends *in vivo*. Nucleic Acid Res 2004;32:255–262. [PubMed: 14715923]

Fechter P, Rudinger J, Giege R, Theobald-Dietrich A. Ribozyme processed tRNA transcripts with unfriendly internal promoter for T7 RNA polymerase: production and activity. FEBS Lett 1998;436:99–103. [PubMed: 9771901]

Frendewey D, Dingermann T, Cooley L, Söll D. Processing of precursor tRNAs in Drosophila. Processing of the 3′ end involves an endonucleolytic cleavage and occurs after 5′ end maturation. J Biol Chem 1985;260:449–454. [PubMed: 3843841]

Ishii R, Minagawa A, Takaku H, Takagi M, Nashimoto M, Yokoyama S. Crystal structure of the tRNA 3′ processing endoribonuclease tRNase Z from Thermotoga maritima. J Biol Chem 2005;280:14138–14144. [PubMed: 15701599]

Kostelecky B, Pohl E, Vogel A, Schilling O, Meyer-Klaucke W. The crystal structure of the zinc phosphodiesterase from *Escherichia coli* provides insight into function and cooperativity of tRNase Z family proteins. J Bacteriol 2006;188:1607–1614. [PubMed: 16452444]

Levinger L, Vasisht V, Greene V, Bourne R, Birk A, Kolla S. Sequence and structure requirements for *Drosophila* tRNA 5′ and 3′ end processing. J Biol Chem 1995;270:18903–18909. [PubMed: 7642547]

Mandel CR, Kaneko S, Zhang H, Gebauer D, Vethantham V, Manley JL, Tong L. Polyadenylation factor CPSF-73 is the pre-mRNA 3′-end-processing endonuclease. Nature 2006;244:953–956. [PubMed: 17128255]

Minagawa A, Takaku H, Takagi M, Nashimoto M. A novel endonucleolytic mechanism to generate the CCA 3′ termini of tRNA molecules in Thermotoga maritima. J Biol Chem 2004;279:15688–15697. [PubMed: 14749326]

Minagawa A, Takaku H, Ishii R, Takagi M, Yokoyama S, Nashimoto M. Identification by Mn^{2+} rescue of two residues essential for the proton transfer of tRNase Z catalysis. Nucleic Acids Res 2006;34:3811–3818. [PubMed: 16916792]

Mohan A, Whyte S, Wang X, Nashimoto M, Levinger L. The 3′ end CCA of mature tRNA is an anti-determinant for eukaryotic 3′-tRNase. RNA 1999;5:245–256. [PubMed: 10024176]

Nashimoto M. Distribution of both length and 5′ terminal nucleotides of mammalian pre-tRNA 3′ trailers reflect properties of 3′ processing endoribonuclease. Nucleic Acids Res 1997;25:1148–1154. [PubMed: 9092623]

Pellegrini O, Nezzar J, Marchfelder A, Putzer H, Condon C. Endonucleolytic processing of CCA-less tRNA precursors by RNase Z in *Bacillus subtilis*. EMBO J 2003;22:4534–4543. [PubMed: 12941704]

Ryan K, Calvo O, Manley JL. Evidence that polyadenylation factor CPSF-73 is themRNA 3′ processing endonuclease. RNA 2004;10:565–73. [PubMed: 15037765]

Schiffer S, Rosch S, Marchfelder A. Assigning a function to a conserved group of proteins: the tRNA 3′-processing enzymes. EMBO J 2002;21:2769–2777. [PubMed: 12032089]

Schilling O, Späth B, Kostelecky B, Marchfelder A, Meyer-Klaucke W, Vogel A. Exosite modules guide substrate recognition in the ZiPD/ElaC protein family. J Biol Chem 2005;280:17857–17862. [PubMed: 15699034]

Spath B, Kirchner S, Vogel A, Schubert S, Meinlschmidt P, Aymanns S, Nezzar J, Marchfelder A. Analysis of the functional modules of the tRNA 3′ endonuclease (tRNase Z). J Biol Chem 2005;280:35440–35447. [PubMed: 16118225]

Takaku H, Minagawa A, Takagi M, Nashimoto M. A candidate prostate cancer susceptibility gene encodes tRNA 3′ processing endoribonuclease. Nucleic Acids Res 2003;31:2272–2278. [PubMed: 12711671]

Tavtigian SV, Simard J, Teng DHF, Abtin V, Baumgard M, Beck A, Camp NJ, Carillo AR, Chen Y, Dayananth P, Desrochers M, Dumont M, et al. A candidate prostate cancer susceptibility gene at chromosome 17p. Nature Genet 2001;27:172–180. [PubMed: 11175785]

Vogel A, Schilling O, Meyer-Klaucke W. Identification of metal binding residues for the binuclear zinc phosphodiesterase reveals identical coordination as glyoxalase II. Biochemistry 2004;43:10379–10386. [PubMed: 15301536]

Vogel A, Schilling O, Spath B, Marchfelder A. The tRNase Z family of proteins: physiological functions, substrate specificity and structural properties. Biol Chem 2005;386:1253–1264. [PubMed: 16336119]

Yan H, Zareen N, Levinger L. Naturally occurring mutations in human mitochondrial pre-tRNA^{Ser} $_{(UCN)}$ can affect the tRNase Z cleavage site, processing kinetics and substrate secondary structure. J Biol Chem 2006;281:3926–3935. [PubMed: 16361254]

Zareen N, Yan H, Hopkinson A, Levinger L. Residues in the conserved His domain of fruit fly tRNase Z that function in catalysis are not involved in substrate recognition or binding. J Mol Biol 2005;350:189–199. [PubMed: 15935379]

Zareen N, Hopkinson A, Levinger L. Residues in two homology blocks on the aminoside of the tRNase Z His domain contribute unexpectedly to pre-tRNA 3′ end processing. RNA 2006;12:1104–1115. [PubMed: 16618969]

(A) Motif II

```
      491              502        508
Dme:  LQAIYVSHLHADHHIGLI
Hsa:  LAAVFVSHLHADHHTGLP
Ath:  LRCIWISHIHADHHTGLA
Cel:  LNCVLITHAHQDHMNGLY
Sce:  IKMIYLSHLHADHHLGII
          S/THxHxDH    G
              •   •  •
      ————————β4—Loop–67————|α2——
Bsu:  IEKIFITHMHGDHVYGLP
Tma:  FKYVFLTHGHVDHIAGLW
Eco:  LDKIFISHLHGDHLFGLP
```

(B) Motif III

```
       583
Dme:   VRHCPNS
Hsa:   VRHCKHA
Ath:   VVHCPQA
Cel:   VHHTRMA
Sce:   AIHCDWA
       v Hc   a
           •
       β8|–140–––––|β9
Bsu:   VIHGVEA
Tma:   TKHVSSE
Eco:   LKHPLEC
```

(C) Motif IV

```
        610
Dme:   YSGDTMP
Hsa:   YSGDTMP
Ath:   YSGDTRP
Cel:   FSGDTKP
Sce:   YSGDTRP
       5SGDT P
           •
       β12|–––211–––|α6
Bsu:   FSGDTRV
Tma:   ISGDSLA
Eco:   IFGDTRP
```

(D) HEAT

```
       630
Dme:   HEAT
Hsa:   HEAT
Ath:   HEAT
Cel:   HEST
Sce:   HEAT
       HEaT
        •
       231
Bsu:   HEAT
Tma:   HECT
Eco:   HEAT
```

(E) HST

```
        646
Dme:   RLKTHSTVSQ
Hsa:   VEKTHSTTSQ
Ath:   VAKNHSTTKE
Cel:   MRKRHSTMGQ
Sce:   VKKKHCTINE
       K  HsT   2
          •
        247
Bsu:   YDYYHSTTEQ
Tma:   RYKNHAAIDE
Eco:   NSRGHSSTRQ
```

(F) Motif V

```
       668
Dme:   THFSQRY
Hsa:   NHFSQRY
Ath:   THFSQRY
Cel:   THFSARY
Sce:   THFSQRY
       tHFSqRY
        •
       269
Bsu:   THISARY
Tma:   YHISTRY
Eco:   THVSSRY
```
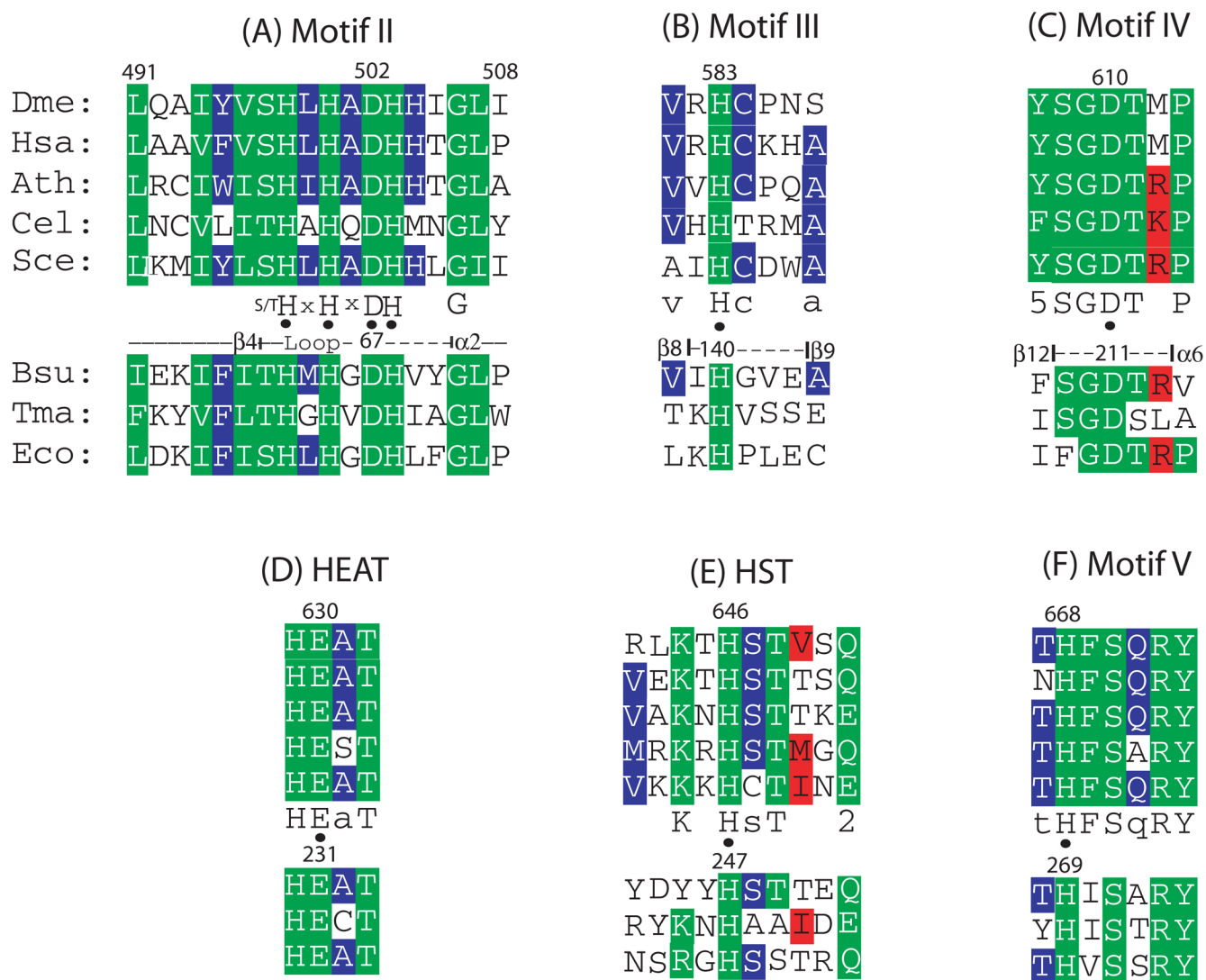
Figure 1. Multiple sequence alignment of conserved loops involved in tRNase Z catalysis
A)Motif II; B) Motif III; C) Motif IV; D) HEAT Loop; E) HST Loop; F) Motif V. The top five aligned sequences are tRNase Z^Ls from *Drosophila melanogaster*, *Homo sapiens*, *Arabidopsis thaliana*, *Caenorhabditis elegans* and *Saccharomyces cerevisiae* (accession numbers Q8MKW7, NP_060597.3, AAM51378, O4476 and NP013005.1, respectively). Numbering of selected residues above the panels is for fruit fly tRNase Z^L (as previously described; Zareen et al., 2005) based on the presumed translation initiation at an internal methionine (r24). Spacing between the homology blocks presented is also conserved in the five tRNase Z^Ls. Designations below the tRNase Z^L panels indicate the consensus and coloring of residues indicates the extent of homology (green: identical; red: conserved in most cases; purple: similar). 3s correspond to the key resdieues in each block (discussed in text). The bottom three sequences are tRNase Z^Ss from *B. subtilis*, *T. maritima* and *E. coli* (accession numbers P54548, NP_228673 and ZP_00726790, respectively). Residue numbers and designations above the bottom panels, based on *Bsu* tRNase Z^S (de la Sierra Gallay et al., 2005), indicate the positions of the secondary structure elements within the loops. The 36 residue gap between Motif III-IV in tRNase Z^L relative to tRNase Z^S is due to the flexible domain which is present at this location in tRNase Z^S and only in the amino half of tRNase Z^L.
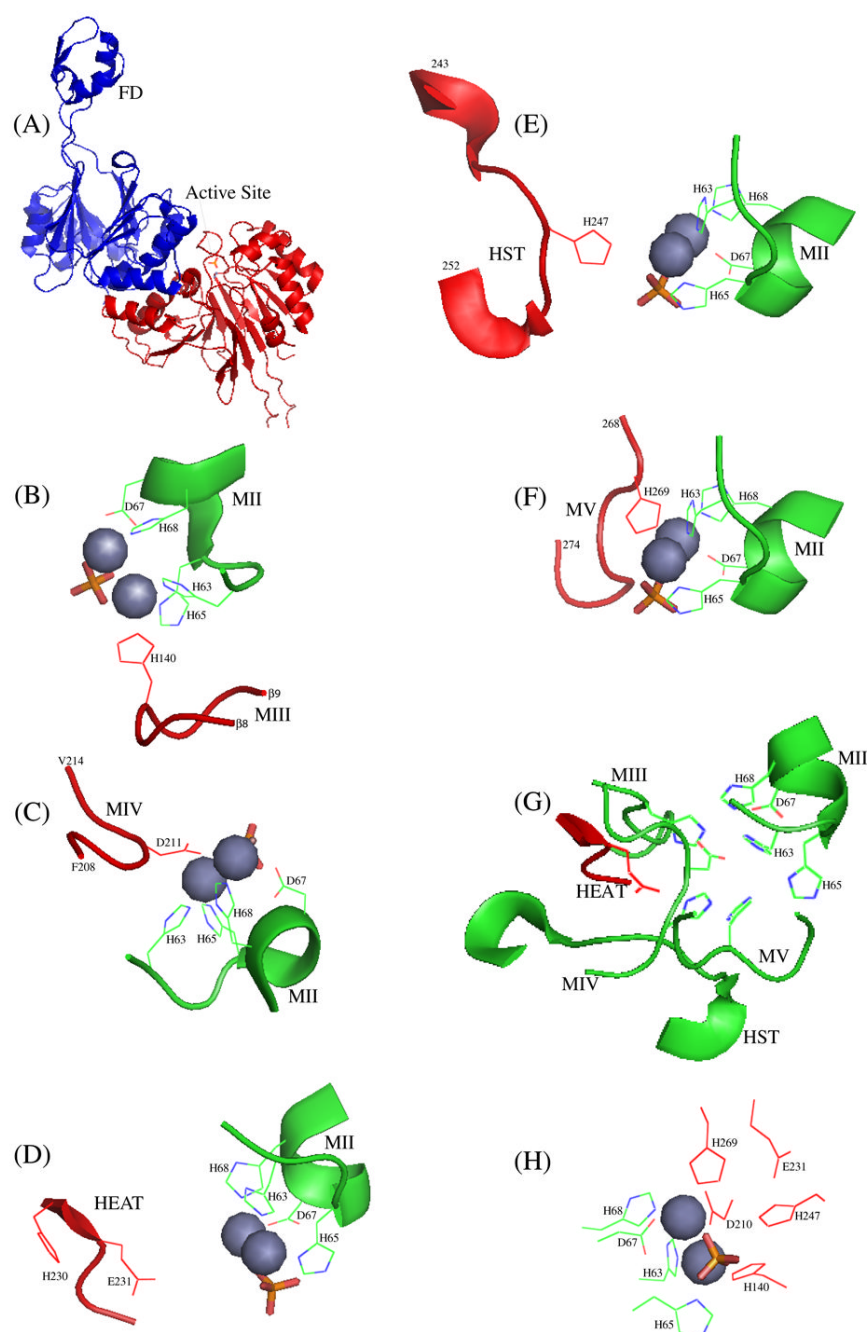
Figure 2. The *Bacillis subtilis* tRNase Z structure model (de la Sierra Gallay et al., 2005; PDB#1Y44), including Motif II and loops on the carboxy side of Motif II, displayed with PyMol (Delano, 2002)

A) Best view of the entire tRNase Z^S structure, a homodimer. The binding subunit (blue, upper left) is characterized by the flexible domain (FD). The active subunit (red, lower right) is dominated by the active site (marked with a fortuitously bound phosphate, orange, in the position suggested by de la Sierra-Gallay et al to be occupied by the scissile phosphodiester linkage in the pre-tRNA substrate). The entrance to the active site appears to be covered by a flap (the PxKxRN loop; Zareen et al., 2006). (B) – (F) Views of each of the loops on the carboxy side of Motif II that are demonstrably important for catalysis. Motif II, two zinc ions (grey

spheres) and the phosphate (orange) that marks the active site are included to provide a frame of reference. These models are presented on the same scale but have been rotated to most clearly display the loops. Relevant side chains are displayed as lines and are labeled with the single letter code for the amino acids (H – His; D – Asp; E – Glu). B) Motif III: His 140 (His 583 in *D. melanogaster*; see alignments in Fig. 1) and the ends of the loop are marked. C) Motif IV: Asp 211 (Asp 610 in *Dme*) and the ends of the loop are marked. D) HEAT: Side chains of His 230 (His 629 in *Dme*) and Glu 231 (Glu 630 in *Dme*) are displayed. Note that Glu 231 is pointing toward His 247 and the active site and His 230 is pointing away from the active site. E) The HST loop: His 247 (His 646 in *Dme*) is displayed and end residues are marked to establish orientation. F) Motif V: His 269 (His 668 in *Dme*) is displayed and ends are marked. G) A composite of the loops from (B) – (F). Motif II is at upper right. Zinc ions and phosphate are omitted. H) Catalytically important residues in tRNase Z. Motif II residues (His 63, His 65, Asp 67, His 68) are at lower left. Side chain of Glu 231 (Glu 630 in *Dme*) is pointing down from upper right, toward His 247. In all the detail views (B – G), a groove or channel occupied by two zincs and a phosphate appears to run between catalytically important signature residues of Motif II (HxHxDH) and the functional elements that approach from the other side (de la Sierra-Gallay et al., 2005).
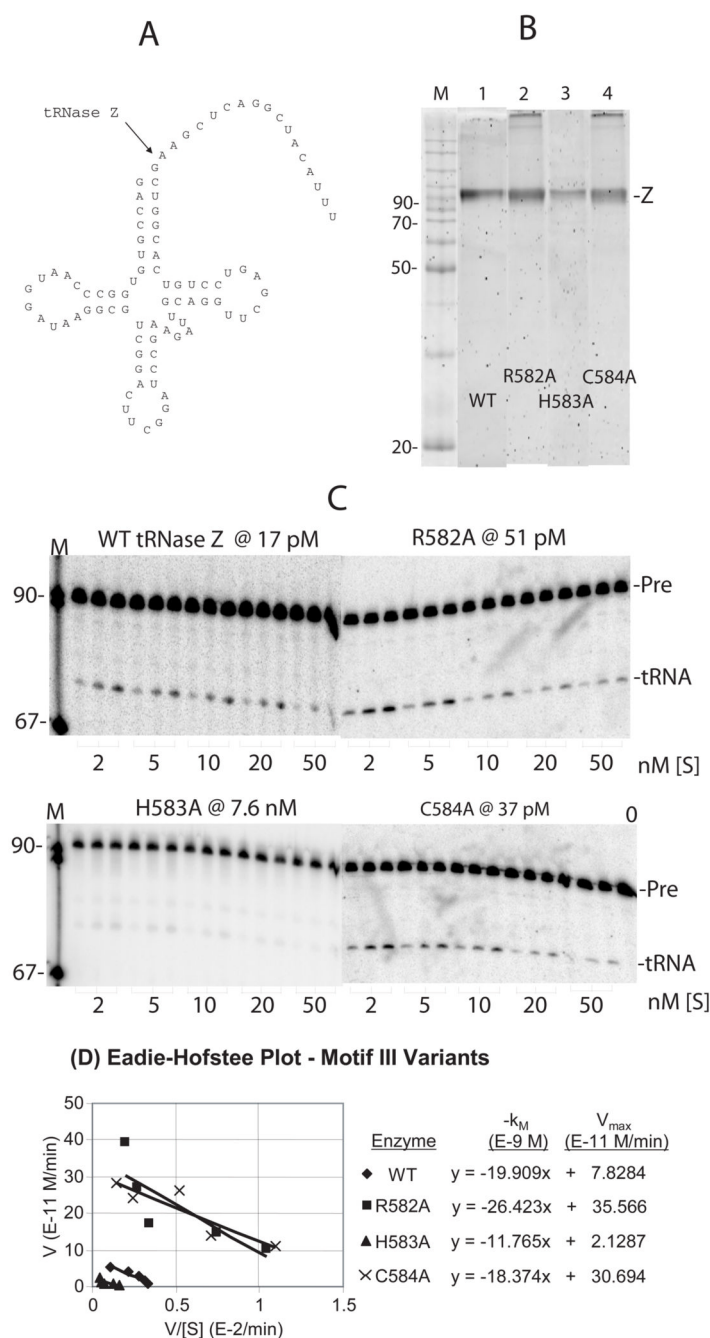
Figure 3. Kinetics of tRNase Z processing
A) Canonical cloverleaf structure and 17 nt 3' end trailer of nuclear-encoded fruit fly pre-tRNA$^{Arg(UCG)}$ substrate (Acc. # AE003494, L09202, nt#1197–1269). The tRNase Z cleavage site following the discriminator base (G73) is marked with an arrow. B) Soluble baculovirus-expressed tRNase Z electrophoresed on a 10% polyacrylamide SDS gel. Wild type and the Motif III variants R582A, H583A and C584A were loaded in lanes 1–4, respectively, as designated below the lanes. M: Invitrogen Benchmark ladder was loaded in the marker lane. Marker sizes are indicated at left. tRNase Z, as designated at right, has an apparent molecular weight of ~90 kD. Protein loads were 2.5 μl of the first dilution (meant to be 200 ng/μL) in a series used in processing experiments (see below) and tRNase Z band intensities (relative to a

known tRNase Z standard, not shown) were used to adjust the value used for enzyme concentration to calculate k_{cat} from V_{max}. C) Michaelis-Menten processing experiments. Reactions with wild type and variant tRNase Z at enzyme concentrations indicated above the panels (as determined from the protein gel lanes in B) were sampled after 5, 10 and 15 min of incubation and electrophoresed on 6% denaturing polyacrylamide gels (brackets below the gels). Reactions were performed with constant labeled substrate and with varying unlabelled substrate concentration over the range from 2–50 nM as indicated below the gel panels. Images were obtained from dried gels using a Typhoon scanner (GE Healthcare) and analyzed with Imagequant software. M – a labeled DNA marker with sizes as indicated at left. –Pre and – tRNA designations at right refer to the precursor and tRNA product (as in A above). D) Superimposed Eadie – Hofstee plots of V/[S] vs. V (values obtained from traces of gel lanes as in (C); see methods). Slope ($-k_M$) for H583A is slightly lower than the others. V_{max} (intercept in equations at right of plot) and [Enzyme] from panel (B) is used to obtain k_{cat} (see Table 1).
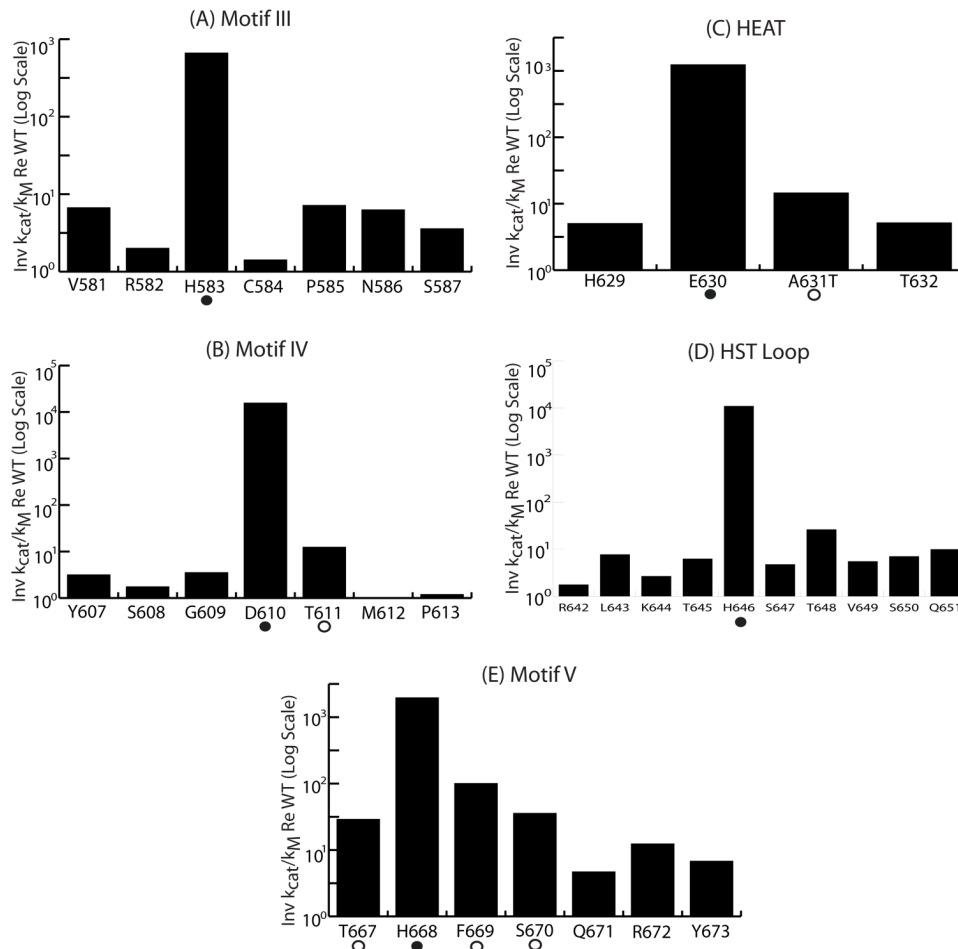
Effect of Substitutions

Figure 4. Bar graphs illustrating the effects of substitutions in conserved regions on the C-side of Motif II

The inverse of k_{cat}/k_M relative to wild type (taken from column 5 in Table 1) is presented on a log scale. Conserved residues (taken from Figure 1A) which affect k_{cat}/k_M are designated with symbols (3 for intermediate reductions and 3 for the greatest reductions). A) The Motif III region; B) the Motif IV region; C) HEAT; D) the HST loop; E) the Motif V region.
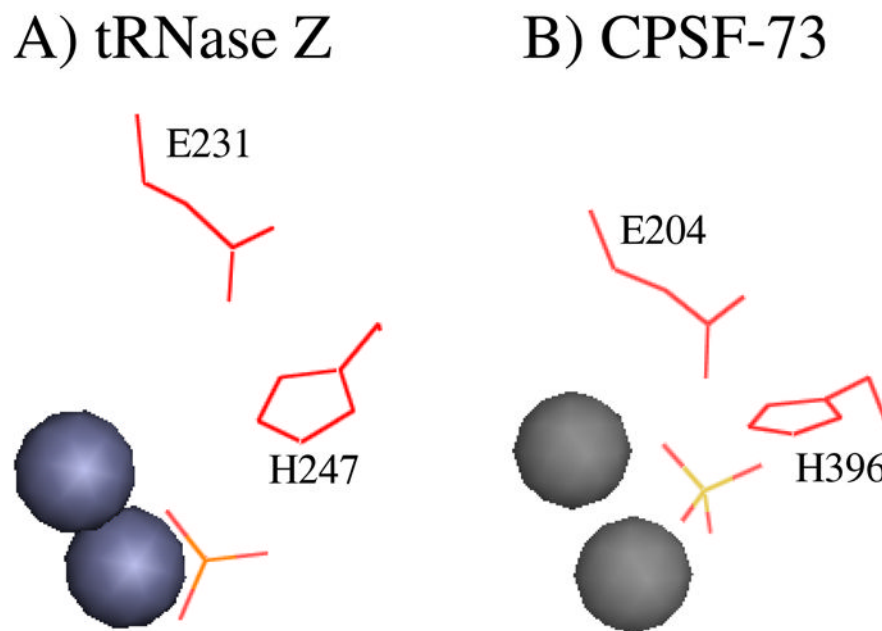
Figure 5. A catalytically important conserved Glu – His contact
A) Glu 231 and His 247 are shown along with spheres corresponding to two zinc ions and a phosphate that marks the active site of tRNase Z (de la Sierra-Gallay et al., 2005; PDB#1Y44). B) The structurally similar placement of Glu 204 and His 396 in human CPSF 73, shown along with spheres corresponding to two zinc ions and a sulfate that marks the active site (Mandel et al., 2006; PDB#2I7T).

TABLE 1

Variant Processing Kinetics

A) Motif III				
1 Enzyme	2 K_{cat} [a]	3 KM [b]	4 K_{cat}/KM [c]	5 Re K_{cat}/KM [d]
WT	5.2 ± 0.73	1.5 ± 0.11	3.36	1
V581	1.56 ± 0.50	2.31 ± 0.29	0.72	0.18
R582	4.63 ± 2.23	2.34 ± 0.27	1.9	0.40
H583	0.006 ± 0.003	1.81 ± 0.63	0.0031	0.0015
C584	5.02 ± 2.54	1.87 ± 0.07	2.74	0.54
P585	0.84 ± 0.22	1.14 ± 0.19	0.72	0.14
N586	0.87 ± 0.03	1.09 ± 0.18	0.82	0.16
S587	1.84 ± 0.20	1.26 ± 0.13	1.46	0.28
B) Motif IV				
1 Enzyme	2 K_{cat} [a]	3 KM [b]	4 K_{cat}/KM [c]	5 Re K_{cat}/KM [d]
Y607	1.84 ± 0.20	2.01 ± 0.19	0.92 ± 0.19	0.31
S608	0.45 ± 0.009	0.25 ± 0.04	1.8 ± 0.36	0.56
G609	0.3 ± 0.05	0.34 ± 0.05	0.92 ± 0.28	0.28
D610	0.00009 ± 0.00002	0.46 ± 0.19	0.00021 ± 0.00004	0.000065
T611	0.26 ± 0.05	0.63 ± 0.20	0.34 ± 0.02	0.11
M612	3.04 ± 1.92	0.89 ± 0.58	3.32 ± 0.67	1.0
P613	1.79 ± 1.15	0.87 ± 0.04	2.12 ± 1.42	0.87
C) HEAT				
1 Enzyme	2 K_{cat} [a]	3 KM [b]	4 K_{cat}/KM [c]	5 Re K_{cat}/KM [d]
H629	0.65 ± 0.21	1.15 ± 0.12	0.59 ± 0.24	0.2
E630	0.0065 ± 0.0007	2.56 ± 1.33	0.0025 ± 0.002	0.00084
A631T	0.37 ± 0.07	1.56 ± 0.32	0.24 ± 0.004	0.072
T632	0.45 ± 0.09	0.74 ± 0.12	0.61 ± 0.05	0.21
D) HST Loop Variant Processing Kinetics				
1 Enzyme	2 K_{cat} [a]	3 KM [b]	4 K_{cat}/KM [c]	5 Re K_{cat}/KM [d]
R642	6.95 ± 3.81	2.78 ± 0.67	2.5	0.56
L643	0.64 ± 0.05	1.29 ± 0.04	0.5	0.13
K644	4.3 ± 0.3	3.15 ± 0.21	1.38	0.37
T645	0.92 ± 0.12	1.55 ± 0.16	0.60	0.16
H646	0.0012 ± 0.0002	3.60 ± 1.14	0.00034	0.000092
S647	1.55 ± 0.48	1.94 ± 0.24	0.78	0.21
T648	0.43 ± 0.15	2.96 ± 0.60	0.14	0.038
V649	0.60 ± 0.005	0.89 ± 0.11	0.69	0.18
S650	1.48 ± 0.25	2.81 ± 0.32	0.52	0.14
Q651	0.88 ± 0.18	2.26 ± 0.42	0.39	0.10
E) Motif V				
1 Enzyme	2 K_{cat} [a]	3 KM [b]	4 K_{cat}/KM [c]	5 Re K_{cat}/KM [d]
T667	0.069 ± 0.026	0.79 ± 0.06	0.086 ± 0.026	0.035
H668	0.0007 ± 0.0003	0.46 ± 0.02	0.0019 ± 0.0011	0.0005
F669	0.01 ± 0.004	0.37 ± 0.14	0.027 ± 0.006	0.01
S670	0.035 ± 0.012	0.98 ± 0.22	0.034 ± 0.005	0.028
Q671	0.22 ± 0.04	0.8 ± 0.39	0.33 ± 0.11	0.22
R672	0.28 ± 0.035	2.64 ± 1.13	0.12 ± 0.04	0.08
Y673	0.12 ± 0.035	0.4 ± 0.03	0.31 ± 0.11	0.15

[a] min^{-1}

[b] $X\ 10^{-8}$ M

[c] $X\ 10^{8}$ M/min

[d] Re K_{cat}/K_M (n-fold reduction) refers to the relative ratio of processing efficiencies: K_{cat}/K_M (variant)/K_{cat}/K_M (wild type) in kinetic experiments with the wild type performed on the same day.

Columns 1–5 are identified in the second row. Averages for k_{cat} (column 2) and K_M (column 3) are presented for two or more Michaelis-Menten experiments with tRNase Z processing of pre-tRNA[Arg] using each of the Motif III variants (Column 1). The values following (+/−) in these two columns are the standard errors. The kinetic values for the wild type are based on 30 experiments including all of the motifs.